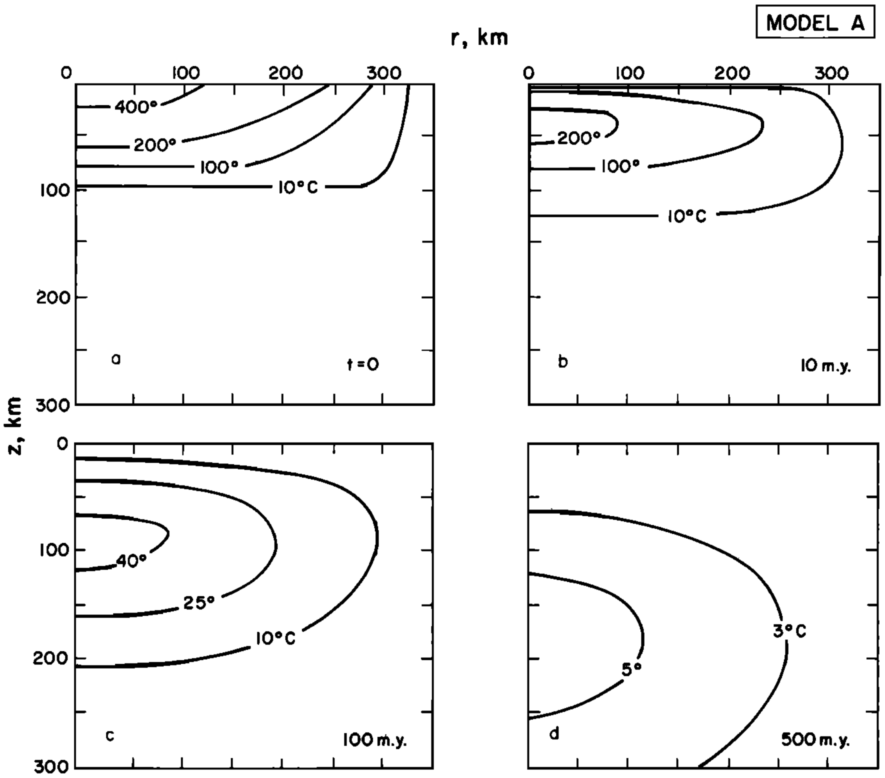

Fig. 10. Basin thermal evolution for model A. The initial field of anomalous temperature ($t = 0$) is that produced only by isotherm uplift. Also shown are the anomalous temperature fields at 10, 100, and 500 m.y. after basin formation.

0.2 km in the first 10 m.y. and an additional 0.2 km during the next 90 m.y. The horizontal distribution of subsidence is controlled by the horizontal extent of uplifted material beneath the basin (Figure 8). By 500 m.y., a region out to 200 km radius has experienced at least 100 m of subsidence.

The amount of subsidence predicted at the center of the basin for model A ($\sim$0.4 km) is about an order of magnitude less than the observed relief of the central basin depression. Even if upper mantle isotherms were raised to the surface during basin formation, the total accumulated subsidence would not exceed 1 km. Thus, if a large portion of the relief associated with the central depression is a consequence of thermal subsidence, an additional source of initial heat is required.

The radial displacement u (Figure 11*c*) is toward the center of the basin. The maximum value occurs between 150 and 200 km radial distance and reaches 200 m by 500 m.y. This value is about half that of the subsidence of the basin center over the same time interval.

In the central basin region both horizontal stresses (Figures 11*b* and 11*d*) are compressional and similar in magnitude. Because σ_{zz} and all shear stresses are zero at the surface, thrust faulting should be the dominant mode of stress release near the center of the basin. Both stress components accumulate most rapidly in the first 10 m.y. and reach 1.6 kbar by 100 m.y. With increasing radial distance r, $\sigma_{\theta\theta}$ approaches zero. In contrast, σ_{rr} becomes extensional at r greater than about 200 km (Figure 11*b*). The zone of maximum extensional σ_{rr} is located between 250 and 350 km radial distance. By 100 m.y., σ_{rr} reaches -0.4 kbar at $r = 290$ km.

As discussed above, fissuring most likely occurred within 100 to 200 m.y. after basin formation and in a stress regime where σ_{rr} was more negative than -0.2 to -0.4 kbar. In model A, the region of the basin where σ_{rr} satisfies this criterion at 100 m.y. is from $r = 230$ to 400 km. Thus while the magnitudes and signs of principal stresses for this model are consistent with fissure formation, the predicted fissures would be at radial distances significantly greater than observed. If fissures originated by thermal stress, we conclude that the anomalous heat contributed by conversion of impact kinetic energy must have been at least comparable in magnitude to that contributed by isotherm uplift. Further, the effects of impact heating were probably concentrated at lesser distance from the basin center than were those of isotherm uplift.

Impact Heating

As discussed above, the magnitude and distribution of impact heating are parameterized by equations (18) and (19) plus a correction for the quantity of impact heat carried away from the excavated cavity by heated ejecta. The crustal structure beneath Orientale (Figure 8) suggests that at least 55 km thickness of shock-heated crust was removed during the excavation of the central portion of the cavity. We have assumed that the uppermost 55 km of the hemispherical distribution of impact heat (equation (18)) was transported outside the basin as hot ejecta. The decay constant s and the net quantity of buried heat E_B remaining beneath the newly formed basin are taken to be free parameters. Following our earlier discussion, we begin by assuming that $E_B = 10^{32}$ erg and we show later the effect of varying this poorly known quantity.

In Figures 12 and 13 are shown the initial distributions of anomalous temperature and the cooling histories predicted by impact heating models for Orientale with $E_B = 10^{32}$ erg and with $s = 25$ km (model B) and 90 km (model C). Most of the initial heat in model B is concentrated within a small volume near the basin surface. The initial anomalous temperature im-